Vol 465|6 May 2010|doi:10.1038/nature08959

LETTERS

Cis-interactions between Notch and Delta generate mutually exclusive signalling states

David Sprinzak[1], Amit Lakhanpal[1], Lauren LeBon[1], Leah A. Santat[1], Michelle E. Fontes[1], Graham A. Anderson[2], Jordi Garcia-Ojalvo[3] & Michael B. Elowitz[1]

The Notch–Delta signalling pathway allows communication between neighbouring cells during development[1]. It has a critical role in the formation of 'fine-grained' patterns, generating distinct cell fates among groups of initially equivalent neighbouring cells and sharply delineating neighbouring regions in developing tissues[2–5]. The Delta ligand has been shown to have two activities: it transactivates Notch in neighbouring cells and *cis*-inhibits Notch in its own cell. However, it remains unclear how Notch integrates these two activities and how the resulting system facilitates pattern formation. Here we report the development of a quantitative time-lapse microscopy platform for analysing Notch–Delta signalling dynamics in individual mammalian cells, with the aim of addressing these issues. By controlling both *cis*- and *trans*-Delta concentrations, and monitoring the dynamics of a Notch reporter, we measured the combined *cis*–*trans* input–output relationship in the Notch–Delta system. The data revealed a striking difference between the responses of Notch to *trans*- and *cis*-Delta: whereas the response to *trans*-Delta is graded, the response to *cis*-Delta is sharp and occurs at a fixed threshold, independent of *trans*-Delta. We developed a simple mathematical model that shows how these behaviours emerge from the mutual inactivation of Notch and Delta proteins in the same cell. This interaction generates an ultrasensitive switch between mutually exclusive sending (high Delta/low Notch) and receiving (high Notch/low Delta) signalling states. At the multicellular level, this switch can amplify small differences between neighbouring cells even without transcription-mediated feedback. This Notch–Delta signalling switch facilitates the formation of sharp boundaries and lateral-inhibition patterns in models of development, and provides insight into previously unexplained mutant behaviours.

Notch and Delta are single-pass transmembrane protein families found in metazoan species. Delta in one cell can bind to, and transactivate, Notch in a neighbouring cell. This interaction results in proteolytic release of the Notch intracellular domain, which translocates to the nucleus and activates target genes[6] (Fig. 1a). Delta also has a second role, inhibiting Notch activity in its own cell (*cis*-inhibition)[7–10]. *Cis*-inhibition has been shown to involve direct interaction of the two proteins[11], but current understanding is incomplete[12].

To understand how concentrations of *cis*- and *trans*-Delta are integrated by the Notch pathway (Fig. 1b), we constructed cell lines that allowed us to modulate the concentrations of *cis*- and *trans*-Delta independently, and to monitor quantitatively the transcriptional response of a Notch reporter (Fig. 1c and Supplementary Fig. 1). These cell lines stably expressed Notch receptors and corresponding yellow fluorescent protein (YFP) reporters of Notch activity (Supplementary Figs 1 and 2). They also contained a doxycycline-inducible chimaeric rat *Dll1–mCherry* fusion gene (Delta–mCherry; Supplementary Fig. 3). In our main cell line, hN1G4^{esn}, the intracellular domain of human NOTCH1 was replaced with a minimal variant of the transcriptional activator Gal4, denoted Gal4^{esn} (ref. 13), to avoid activation of endogenous Notch targets[14–16]. A second cell line, hN1, containing the full-length human NOTCH1 was analysed as a control (Supplementary Fig. 1). Notch messenger RNA expression levels in these cells were comparable to those observed in early T-cell progenitors where Notch is active[17] (Supplementary Information).

We first asked how Notch activity depends on the concentration of *trans*-Delta. We adsorbed fusion proteins, consisting of immunoglobin-G (IgG) fused to the extracellular domain of human

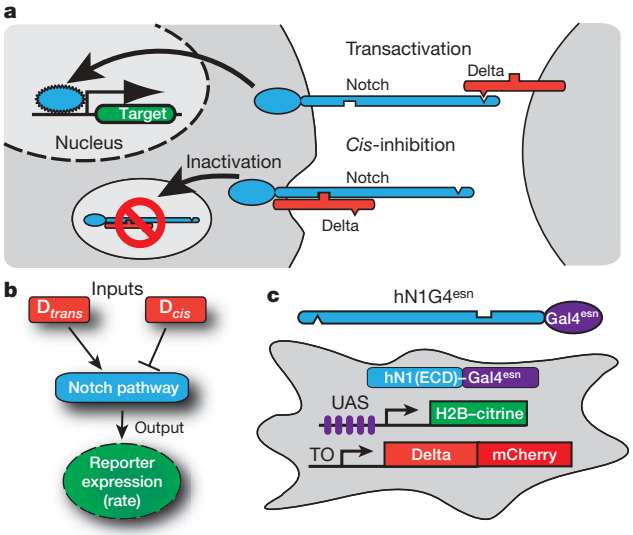

Figure 1 | System for analysing signal integration in the Notch–Delta pathway. a, Notch (blue) and Delta (red) interactions are indicated schematically. **b**, Notch activity integrates *cis*-and *trans*-Delta. **c**, T-REx-CHO-K1 cell line for analysing Notch activity. The hN1G4^{esn} cell line stably incorporates a variant of human NOTCH1 in which the activator Gal4^{esn} replaces the Notch intracellular domain (here hN1(ECD) is the extracellular domain of hN1). This cell line also contains genes for histone 2B (H2B)–citrine (YFP) reporter controlled by an upstream activating sequence (UAS) promoter, a tetracycline-inducible (TO) Delta–mCherry fusion protein and a constitutively expressed H2B–cerulean (cyan fluorescent protein, or CFP) for image segmentation (not shown). A similar cell line expressing full-length human NOTCH1 (the hN1 cell line) was also analysed (Supplementary Figs 1 and 2). These cells exhibit no detectable endogenous Notch or Delta activities. Notch–Delta interactions are indicated schematically and do not represent molecular interaction mechanisms[11].

[1]Howard Hughes Medical Institute, Division of Biology and Department of Applied Physics, California Institute of Technology, 1200 East California Boulevard, Pasadena, California 91125, USA. [2]Department of Chemical and Systems Biology, Stanford University School of Medicine, 269 Campus Drive, Stanford, California 94305, USA. [3]Department de Física i Enginyeria Nuclear, Universitat Politècnica de Catalunya, Colom 11, E-08222 Terrassa, Spain.

DLL1 (Delta^{ext}), to the surface of plates at different concentrations, denoted D_{plate} (Fig. 2a and Supplementary Fig. 4)[18,19], and recorded time-lapse movies of Notch activation. Before the start of each movie ($t < 0$), we inhibited Notch activation using the γ-secretase inhibitor *N*-[*N*-(3,5-difluorophenacetyl)-L-alanyl]-*S*-phenylglycine *t*-butyl ester (DAPT). At $t = 0$, DAPT was washed out, allowing the fluorescent reporter to accumulate at a rate determined by Notch activity (Fig. 2b, c and Supplementary Movie 1). The YFP production rate showed a graded response to D_{plate}, well-fitted by a Hill function with a modest Hill coefficient (Fig. 2d). A similar response was observed in the hN1 cell line (Supplementary Figure 1). This graded response was not due to the use of plate-bound ligands: when cells expressing only Delta were co-cultured with cells expressing only Notch, we observed a similarly graded dependence of Notch activity on the level of Delta expression, but with greater variability (Supplementary Fig. 5).

We next set out to quantify the response of Notch to varying concentrations of *cis*-Delta in the hN1G4^{esn} cell line. We used a scheme in which Delta–mCherry was expressed in a pulse before the start of the movie and subsequently allowed to dilute, effectively titrating its concentration[20] (Fig. 3a). These experiments were performed at low cell density, where relatively weak intercellular activation of Notch is observed (Supplementary Fig. 6), and transactivation was induced predominantly by D_{plate}. At the beginning of the movie,

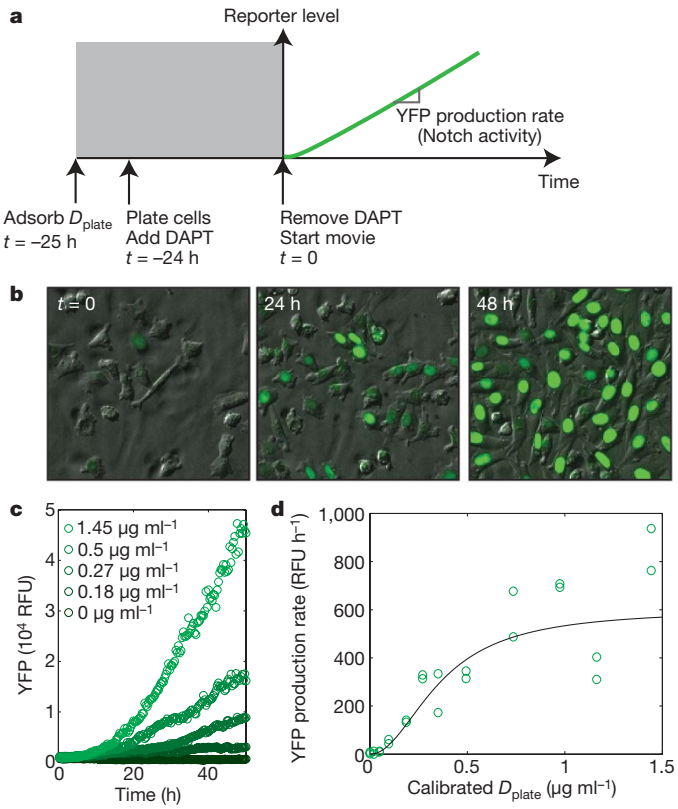

Figure 2 | Transactivation of Notch occurs in a graded fashion. **a**, Experimental design. The rate of increase of fluorescence (slope of green line) is a measure of Notch activity. **b**, Typical hN1G4^{esn} filmstrip showing activation of Notch reporter (green), with $D_{plate} = 1.16\ \mu g\ ml^{-1}$ and frame times as indicated (Supplementary Movie 1; compare with Supplementary Fig. 6). **c**, hN1G4^{esn} cells respond in a graded manner to variations in D_{plate}. The data show the median fluorescence of individual cells within a single field of view for the indicated values of D_{plate} (see Supplementary Fig. 15 for distributions). RFU, relative fluorescence unit. **d**, The relationship between D_{plate} and Notch activity (in RFU per hour, from the linear regime in **c**). The Hill-function fit is indicated by the black line, which has Hill coefficient $n = 1.7$ (95% confidence interval, $n = 0.8$–2.7). Similar results were obtained using the hN1 cell line (Supplementary Fig. 1). We note that doxycycline does not directly affect Notch activation or cell growth, nor does D_{plate} affect cell growth (Supplementary Fig. 12).

Notch reporter expression was fully inhibited by high Delta–mCherry concentrations (Fig. 3b and Supplementary Movie 2). Subsequently, Delta–mCherry concentrations gradually declined on a timescale of $\tau_D = 32 \pm 2.5$ h, consistent with dilution by cell growth and division (Fig. 3c). At $t_{on} \approx 40$ h, we observed a sharp onset of reporter expression in the median response of the population (Fig. 3c). Even sharper responses were evident in individual cell lineages (Fig. 3d–f and Supplementary Fig. 13). Similar behaviour was observed in the hN1 cell line (Supplementary Fig. 7).

To quantify the sharpness of *cis*-inhibition, we computed the rise time, denoted τ_{rise}, required for Notch activity to increase by a factor of e in individual cells (Fig. 3e and Fig. 3a, inset). The distribution of τ_{rise} showed a median of 2.6 h, which is considerably less than τ_D (Fig. 3f). For comparison, an equivalently sharp Hill function of *cis*-Delta would require a Hill coefficient of $\tau_D/\tau_{rise} \approx 12$.

We repeated the experiment for a variety of D_{plate} values, allowing us to directly measure the integrated response of Notch across the two-dimensional input space of *cis*- and *trans*-Delta concentrations (Fig. 3g and Supplementary Fig. 14). Activation occurred at a similar value of t_{on} and, therefore, a similar *cis*-Delta concentration, regardless of D_{plate}, as indicated by the fixed position of the transition from black to green points in Fig. 3g. In addition, the activation remained sharp at all D_{plate} values for which it could be clearly measured.

Thus, an explanation for the observed *cis*- and *trans*-signal integration must simultaneously account for the three key features of the experimental data: a graded response to *trans*-Delta (Fig. 2d), a sharp response to *cis*-Delta (Fig. 3c–f) and a fixed threshold for *cis*-inhibition across varying concentrations of *trans*-Delta (Fig. 3g). We show here that a simple model can explain these observations in a unified way (Box 1 and Fig. 3h). The model's key assumption is that Notch and Delta in the same cell mutually inactivate each other. As shown in Box 1, strong enough mutual inactivation can produce an ultrasensitive switch between two mutually exclusive signalling states: cells can be in a predominantly 'sending' state, with high Delta concentration and low Notch concentration, or a 'receiving' state, with high Notch concentration and low Delta concentration, but cannot be in both states at the same time. Alternative models that do not include mutual inactivation fail to account for the observed data (Supplementary Fig. 8).

The three features described above emerge naturally in this model. First, in the absence of *cis*-Delta, the rate of Notch activation is proportional to the *trans*-Delta concentration, generating a graded response. Second, a sharp response to *cis*-Delta results from mutual inactivation, which causes an excess of either protein to strongly diminish the activity of the other. Finally, the switching point occurs when Notch and *cis*-Delta concentrations are comparable, and is therefore only weakly dependent on *trans*-Delta.

The mutual-inactivation model predicts *cis*-inhibition, not just of Notch by Delta but also of Delta by Notch. This interaction is supported by results in other systems[12,21,22]. We tested this prediction in our system using a transactivation assay based on co-culture of Delta-expressing sending cells with Notch reporter cells. Expression of Notch in the Delta-expressing cells reduced their ability to transactivate, as predicted (Supplementary Fig. 9). The exact biochemical mechanism of mutual inactivation remains unclear, but we observed no sharp drop in the total cellular Delta–mCherry fluorescence during switching, suggesting that the inactive complex may be stable in these conditions (Fig. 3c, d).

This signalling switch has important implications for multicellular patterning. To understand these implications, consider two neighbouring cells that produce Notch and Delta at constant rates (Fig. 4a). A slight excess of Notch production in one cell and a slight excess of Delta production in its neighbour can generate a strong signalling bias in one direction: the first cell becomes a receiver and the second becomes a sender. In this way, a small difference in production rates between cells is amplified into a much larger difference in Notch activity (Fig. 4b). This amplification does not require transcriptional regulation or feedback.

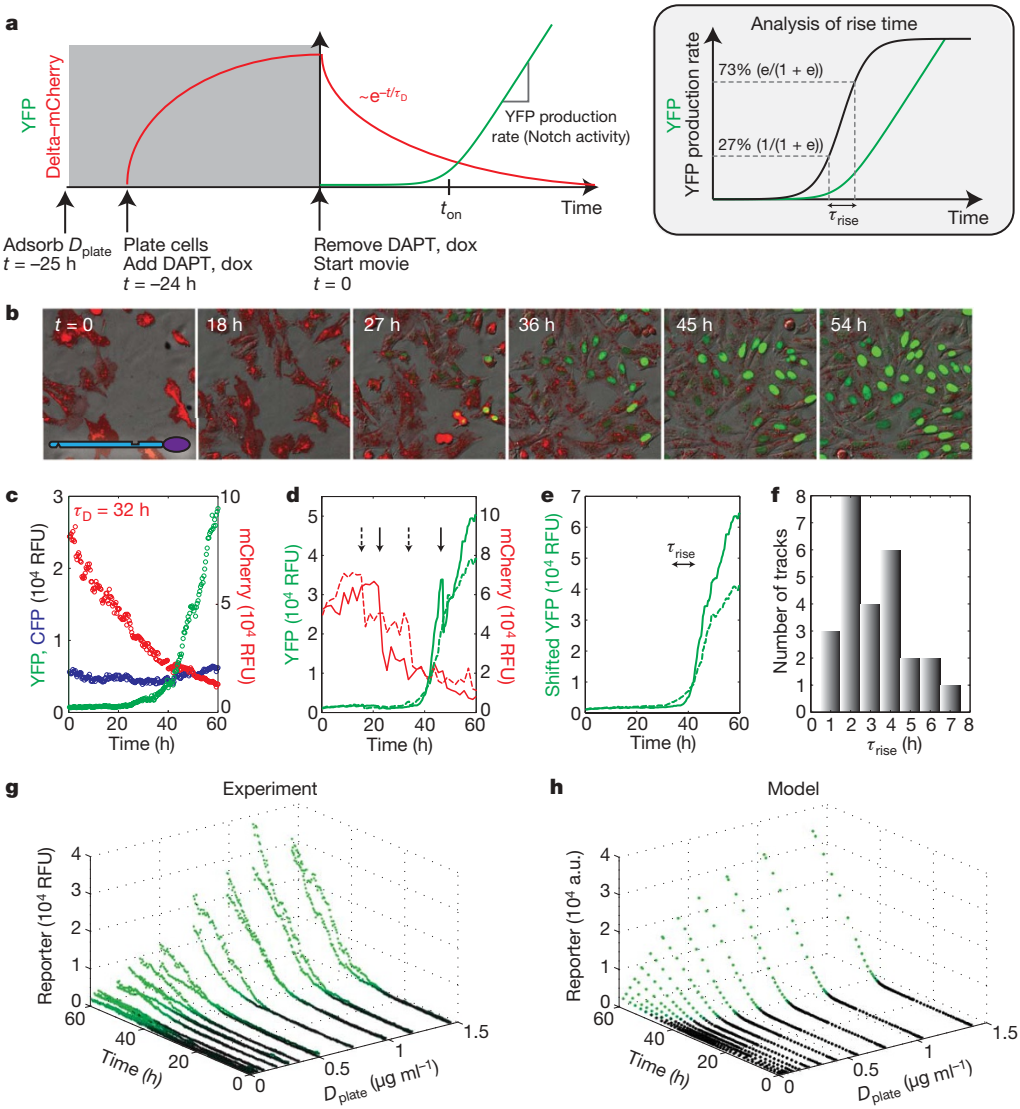

Figure 3 | *Cis–trans* signal integration by Notch. **a**, Experimental protocol. Inset, the rise time, τ_{rise}, is the time required for Notch activity (black line or slope of green line) to change by a factor of e. dox, doxycycline. **b**, Filmstrip of hN1G4^{esn} cells, with $D_{plate} = 1.45\ \mu g\ ml^{-1}$ (Supplementary Movie 2), showing Delta–mCherry fluorescence (red) and concomitant activation of Notch reporter (green) at the indicated times (compare with Supplementary Fig. 6). **c**, Population average (median) response for the same movie shows a slow decay of Delta–mCherry fluorescence (red data), but a sharp response of reporter expression (green data). Constitutively expressed pCMV–H2B–cerulean (blue data) remains constant (control). Compare with the single-cell tracks in Supplementary Fig. 13 and the response to modulation of doxycycline in Supplementary Fig. 14. **d**, Single-cell response for two individual cells (solid and dashed lines, colours as in **c**). Black arrows mark cell divisions. **e**, Single-cell traces in **d** replotted, but shifted up after each cell division event to 'add back' sister-cell fluorescence, to show the continuity of Notch activity (see also Supplementary Fig. 13). **f**, Histogram of τ_{rise} from 26 non-overlapping cell lineages (Supplementary Fig. 13). **g**, Notch response to both *cis*- and *trans*-Delta. Data shown are from two duplicate movies acquired at each of 12 D_{plate} values for hN1G4^{esn} cells. Green colouring indicates data that exceed a detection threshold. Note that onset (the black-to-green transition) occurs at approximately the same time for all D_{plate} values. **h**, Simulations based on the model in Box 1 are qualitatively similar to data in **g** (see Supplementary Information and Supplementary Fig. 16 for model details). a.u., arbitrary units.

The send–receive signalling switch can facilitate formation of sharp boundaries. For example, in *Drosophila* Notch and Delta sharply delineate wing vein boundaries[4,5]. In this system, Delta production is initially expressed in a graded profile transverse to the vein. Eventually, Notch signalling is restricted to two sharp side bands on either side of the vein axis.

As a simplified model, we simulated the development of a field of cells with a graded rate of Delta production and a uniform rate of Notch production (Fig. 4c). The mutual-inactivation model generated sharply defined side bands of Notch signalling at positions where the two production rates intersect, that is, where sender and receiver cells are next to each other (Fig. 4c). Moreover, this model explains a striking mutant behaviour that occurs in the *Drosophila* wing vein system. Although Notch and Delta are individually haploinsufficient (causing thicker veins), the *Notch*$^{+/-}$ *Delta* $^{+/-}$ double mutant restores the wild-type phenotype[23]. This suppression of the single-mutant phenotypes in the double mutant emerges automatically in the model because proportional rescaling of the Notch and Delta production rates does not move their intersection points (Fig. 4d). This suppression is maintained across a broad range of parameter values and persists even with additional feedbacks (Supplementary Fig. 10c), but is difficult to explain in other models (Supplementary Fig. 10a and Supplementary Information).

The send–receive signalling switch can also facilitate lateral-inhibition patterning. When Notch transcriptionally downregulates Delta expression, the resulting intercellular positive-feedback loop can generate 'checkerboard' patterns of Notch activity[24,25] (Fig. 4e). Without mutual inactivation, pattern formation requires a minimum Hill coefficient of

Box 1 | Model of mutual inactivation of Notch and Delta

Here we describe a simple model of Notch–Delta interactions that explains the experimental data and provides insight into developmental patterning processes. The model involves several reactions. First, during intercellular signalling, Notch in one cell binds to extracellular Delta, of concentration D_{trans}, leading to release of the Notch intracellular domain and degradation of its extracellular domain[6]. Similarly, Notch in a neighbouring cell, N_{trans}, can bind to Delta. Second, Notch binds irreversibly to Delta in the same cell to form a stable, inactive, complex, which is effectively removed from the system[12]. Finally, Notch and Delta are produced at constant rates, and degraded and/or diluted at a constant rate, in addition to being removed through the interactions described above.

These reactions can be expressed as a set of ordinary differential equations for the concentrations of free Notch, N, and free Delta, D, in an individual cell. An additional equation represents the intracellular domain of Notch, S, which activates expression of the fluorescent reporter gene:

$$\frac{dN}{dt} = \beta_N - \gamma N - \frac{DN}{k_c} - \frac{D_{trans}N}{k_t}$$

$$\frac{dD}{dt} = \beta_D - \gamma D - \frac{DN}{k_c} - \frac{DN_{trans}}{k_t}$$

$$\frac{dS}{dt} = \frac{D_{trans}N}{k_t} - \gamma_S S$$

Here D_{trans} represents D_{plate} in Figs 2 and 3, but could also represent Delta concentration in one or more neighbouring cells (Supplementary Information). Similarly, D in these equations corresponds to *cis*-Delta in the experiments, and β_N and β_D denote the production rates of Notch and Delta, respectively. The combined degradation and dilution rate, γ, is assumed for simplicity to be the same for Notch and Delta, and γ_S is the rate of decay of S. We write k_c and k_t to denote the strengths of *cis*-inhibition and transactivation, respectively. See Supplementary Information for a more detailed description.

In the steady state, mutual inactivation leads to a switch between two qualitatively distinct behaviours, depending on the relative production rates of Delta and Notch. When $\beta_D > \beta_N$, excess Delta effectively inactivates almost all Notch, allowing cells to send, but not efficiently receive, signals. Conversely, when $\beta_D < \beta_N$, excess Notch effectively inactivates Delta, allowing cells to receive, but not efficiently send, signals. Thus, the system approaches two mutually exclusive signalling states: high Delta/low Notch ('sending'; pink shading in Figure), and high Notch/low Delta ('receiving'; blue shading in Figure). We note that this switch is not bistable.

In the steady state, the transition between the two regimes is ultrasensitive: near the threshold, a relatively small change in β_D or β_N can lead to a much larger change in signalling (Supplementary Fig. 11). Related biochemical kinetics occur in bacterial small RNA and protein sequestration[27–29]. In Fig. 3, ultrasensitivity occurs dynamically in response to the decay of the total Delta concentration (Supplementary Information).

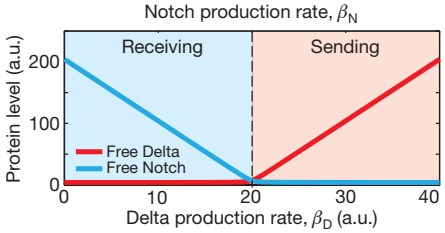

$n = 2$, or higher, in the regulatory feedback loop (Fig. 4f, left, and Supplementary Information). Although we cannot rule out such cooperativity, or additional feedback loops, no evidence for strongly cooperative transactivation was observed here or previously (Fig. 2d and Supplementary Fig. 1). In contrast, mutual inactivation allows patterning even without cooperativity, by introducing a sharp response to changes in Delta expression (Fig. 4f, right). In addition, for strong enough *cis*-inhibition, mutual inactivation allows cells with high Delta concentrations to coexist next to one another in the steady state, leading

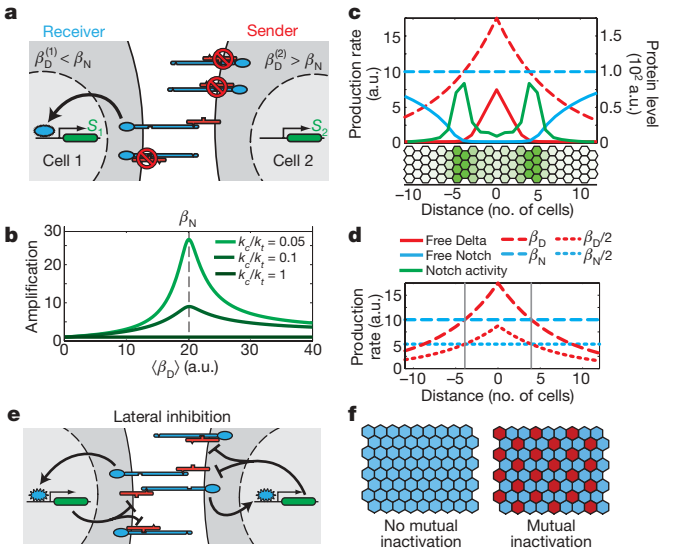

Figure 4 | The mutual-inactivation model in multicellular patterning. **a**, Signal amplification. The two interacting cells have the same amount of Notch (here, two molecules) but different amounts of Delta (one or three molecules). Owing to the *cis*-interaction between Notch and Delta, signalling is strongly biased to cell 1. **b**, Notch amplifies differences between cells. Signal amplification, $(S_1/S_2 - 1)/(\beta_D^{(2)}/\beta_D^{(1)} - 1)$, for two interacting cells, with different Delta production rates, $\beta_D^{(2)} = 1.35\beta_D^{(1)}$ (see model in Supplementary Information). The x axis shows the average Delta production rate, $\langle\beta_D\rangle = (\beta_D^{(2)} + \beta_D^{(1)})/2$. Maximum amplification occurs when Delta production rates flank β_N (vertical dashed line). Stronger mutual inactivation (smaller k_c/k_t) increases signal amplification. **c**, **d**, Sharp boundary formation in response to a gradient of Delta production. **c**, Simulation of a field of interacting cells in which Delta production rates decay exponentially from the centre, according to $\beta_D(x) = \beta_D^0 \exp(-x/x_0)$ with $x_0 = 7$ cells (dashed red line). The Notch production rate, β_N, is constant (dashed blue line). The resulting free Notch and Delta protein levels are indicated (solid lines). Notch activation occurs in two sharply defined columns of cells (green line in plot and green cells in cellular diagram). **d**, Suppression of mutant phenotypes is explained by the mutual-inactivation model. Grey lines indicate positions where $\beta_N = \beta_D(x)$, leading to Notch activity peaks. Simultaneous reduction of both Notch and Delta production rates by half maintains boundary positions (dotted lines) (Supplementary Fig. 10). **e**, **f**, Mutual inactivation facilitates lateral-inhibition patterning (**e**). In the absence of cooperativity in regulatory feedback, a standard lateral-inhibition model[24] cannot pattern (**f**, left) but a model of lateral inhibition with mutual inactivation can (**f**, right).

to a broader range of possible patterns (Supplementary Fig. 17). Finally, we note that low concentrations of free Notch and Delta exist in sender and, respectively, receiver cells for finite mutual-inactivation strengths (Supplementary Fig. 11). The resulting signalling between like cells (senders or receivers) can have a role in lateral-inhibition patterning dynamics.

Different signal-transduction pathways are optimized to encode and transmit information in different ways, depending on the tasks they perform in the organism. Our results show that mutual inactivation between Notch and Delta in the same cell forces cells into predominantly sending or receiving states (Box 1 Figure). In a multicellular context, this mechanism amplifies small initial differences between neighbouring cells, and facilitates pattern formation (Fig. 4). This signalling switch thus seems to optimize the Notch–Delta pathway for directional signalling, and may explain why it is used in specific developmental processes. Moreover, this mechanism could also provide other advantages, such as faster dynamics[26,27]. We note that interactions between Notch and Delta are typically embedded in more-complex dynamic regulatory networks that involve additional feedbacks. It will be important to explore how this signalling switch functions in the context of larger regulatory circuits.

METHODS SUMMARY

We assembled genetic constructs and cell lines by standard methods (Supplementary Table 1). All cell lines used in the main text (Supplementary Table 2) were derived from T-REx-CHO-K1 (Invitrogen). Cell lines were constructed by sequential rounds of Lipofectamine 2000 (Invitrogen) transfection and selection. We isolated stably transfected clones by limiting dilution or FACS.

Time-lapse microscopy was performed with cells plated on 24-well glass-bottom plates (MatTek). For plate-bound Delta experiments, IgG–Delta^{ext} was adsorbed to the plate together with 5 μg ml^{-1} hamster fibronectin (Innovative Research) before cell plating. Before imaging, cells were switched to a low-fluorescence medium, consisting of 5% FBS in αMEM lacking riboflavin, folic acid, phenol red and vitamin B12. Movies were acquired using an Olympus IX81-ZDC microscope, equipped with an environmental chamber at 37 °C supplying 5% CO_2, a ×20, numerical-aperture-0.7 objective, and automated acquisition software (METAMORPH (version 7.5.6.0), Molecular Devices).

We obtained western blots for Gal4 using standard protocols. Blots were probed using rabbit anti-Gal4 DBD primary antibody (sc-577, Santa Cruz Biotechnology; 1:200) followed by incubation with horseradish peroxidase-labelled anti-rabbit IgG secondary antibody (Amersham; 1:2,000). Bands were quantified using a VersaDoc gel imaging system (Bio-Rad). Quantitative PCR with reverse transcription was performed using standard protocols based on the RNeasy kit (Qiagen) and the iScript cDNA synthesis kit (Bio-Rad).

We analysed co-culture experiments for YFP fluorescence using a FACScalibur flow cytometer (Becton Dickinson) and standard protocols. Movies were analysed in several stages. First, individual cell nuclei were identified in CFP images using a custom algorithm (MATLAB, MathWorks R2007a) based on edge detection and thresholding of constitutively expressed H2B–cerulean fluorescence. Then, for analysis of single-cell expression trajectories, individual nuclei were tracked across frames using custom software (MATLAB, C) based on the softassign algorithm (Supplementary Information). All single-cell trajectories were validated manually. For further details, see Supplementary Information.

Full Methods and any associated references are available in the online version of the paper at www.nature.com/nature.

Received 27 April 2009; accepted 26 February 2010.
Published online 25 April 2010.

1. Artavanis-Tsakonas, S., Rand, M. D. & Lake, R. J. Notch signaling: cell fate control and signal integration in development. *Science* **284,** 770–776 (1999).
2. Goodyear, R. & Richardson, G. Pattern formation in the basilar papilla: evidence for cell rearrangement. *J. Neurosci.* **17,** 6289–6301 (1997).
3. Heitzler, P. & Simpson, P. The choice of cell fate in the epidermis of *Drosophila*. *Cell* **64,** 1083–1092 (1991).
4. Huppert, S. S., Jacobsen, T. L. & Muskavitch, M. A. Feedback regulation is central to Delta-Notch signalling required for *Drosophila* wing vein morphogenesis. *Development* **124,** 3283–3291 (1997).
5. de Celis, J. F., Bray, S. & Garcia-Bellido, A. Notch signalling regulates veinlet expression and establishes boundaries between veins and interveins in the *Drosophila* wing. *Development* **124,** 1919–1928 (1997).
6. Bray, S. J. Notch signalling: a simple pathway becomes complex. *Nature Rev. Mol. Cell Biol.* **7,** 678–689 (2006).
7. de Celis, J. F. & Bray, S. Feed-back mechanisms affecting Notch activation at the dorsoventral boundary in the *Drosophila* wing. *Development* **124,** 3241–3251 (1997).
8. Micchelli, C. A., Rulifson, E. J. & Blair, S. S. The function and regulation of cut expression on the wing margin of *Drosophila*: Notch, Wingless and a dominant negative role for Delta and Serrate. *Development* **124,** 1485–1495 (1997).
9. Klein, T., Brennan, K. & Arias, A. M. An intrinsic dominant negative activity of serrate that is modulated during wing development in *Drosophila*. *Dev. Biol.* **189,** 123–134 (1997).
10. Miller, A. C., Lyons, E. L. & Herman, T. G. cis-Inhibition of notch by endogenous delta biases the outcome of lateral inhibition. *Curr. Biol.* **19,** 1378–1383 (2009).
11. Cordle, J. *et al.* A conserved face of the Jagged/Serrate DSL domain is involved in Notch *trans*-activation and *cis*-inhibition. *Nature Struct. Mol. Biol.* **15,** 849–857 (2008).
12. Matsuda, M. & Chitnis, A. B. Interaction with Notch determines endocytosis of specific Delta ligands in zebrafish neural tissue. *Development* **136,** 197–206 (2009).
13. Kakidani, H. & Ptashne, M. GAL4 activates gene expression in mammalian cells. *Cell* **52,** 161–167 (1988).
14. Struhl, G. & Adachi, A. Nuclear access and action of notch *in vivo*. *Cell* **93,** 649–660 (1998).
15. Aster, J. C. *et al.* Essential roles for ankyrin repeat and transactivation domains in induction of T-cell leukemia by notch1. *Mol. Cell. Biol.* **20,** 7505–7515 (2000).
16. Yang, L. T. *et al.* Fringe glycosyltransferases differentially modulate Notch1 proteolysis induced by Delta1 and Jagged1. *Mol. Biol. Cell* **16,** 927–942 (2005).
17. Rothenberg, E. V., Moore, J. E. & Yui, M. A. Launching the T-cell-lineage developmental programme. *Nature Rev. Immunol.* **8,** 9–21 (2008).
18. Varnum-Finney, B. *et al.* Immobilization of Notch ligand, Delta-1, is required for induction of notch signaling. *J. Cell Sci.* **113,** 4313–4318 (2000).
19. Wang, S. *et al.* Notch receptor activation inhibits oligodendrocyte differentiation. *Neuron* **21,** 63–75 (1998).
20. Rosenfeld, N., Young, J. W., Alon, U., Swain, P. S. & Elowitz, M. B. Gene regulation at the single-cell level. *Science* **307,** 1962–1965 (2005).
21. Jacobsen, T. L., Brennan, K., Arias, A. M. & Muskavitch, M. A. Cis-interactions between Delta and Notch modulate neurogenic signalling in *Drosophila*. *Development* **125,** 4531–4540 (1998).
22. Shaye, D. D. & Greenwald, I. LIN-12/Notch trafficking and regulation of DSL ligand activity during vulval induction in *Caenorhabditis elegans*. *Development* **132,** 5081–5092 (2005).
23. de Celis, J. F. & Bray, S. J. The Abruptex domain of Notch regulates negative interactions between Notch, its ligands and Fringe. *Development* **127,** 1291–1302 (2000).
24. Collier, J. R., Monk, N. A., Maini, P. K. & Lewis, J. H. Pattern formation by lateral inhibition with feedback: a mathematical model of Delta-Notch intercellular signalling. *J. Theor. Biol.* **183,** 429–446 (1996).
25. Plahte, E. Pattern formation in discrete cell lattices. *J. Math. Biol.* **43,** 411–445 (2001).
26. Melen, G. J., Levy, S., Barkai, N. & Shilo, B. Z. Threshold responses to morphogen gradients by zero-order ultrasensitivity. *Mol. Syst. Biol.* **1,** doi:10.1038/msb4100036 (2005).
27. Levine, E., Zhang, Z., Kuhlman, T. & Hwa, T. Quantitative characteristics of gene regulation by small RNA. *PLoS Biol.* **5,** e229 (2007).
28. Buchler, N. E. & Louis, M. Molecular titration and ultrasensitivity in regulatory networks. *J. Mol. Biol.* **384,** 1106–1119 (2008).
29. Lenz, D. H. *et al.* The small RNA chaperone Hfq and multiple small RNAs control quorum sensing in *Vibrio harveyi* and *Vibrio cholerae*. *Cell* **118,** 69–82 (2004).

Supplementary Information is linked to the online version of the paper at www.nature.com/nature.

Acknowledgements We would like to thank I. Bernstein for the IgG-Delta^{ext}, U. Lendahl for the 12xCSL reporter construct, J. Aster for human NOTCH1 and other constructs, and G. Weinmaster for the rat DLL1 construct and advice. We also thank R. Tsien and K. Thorn for mCherry, S. Megason and S. Fraser for H2B–citrine and other constructs, R. Diamond and D. Perez for assistance with FACS, and F. Tan and J. Yong for help with cloning some of the constructs. We thank A. Eldar, J. Locke, G. Seelig, R. Kishony, B. Shraiman, A. C. Oates and members of the Elowitz laboratory for discussions and advice. This work was supported by the US National Institutes of Health Fellowship F32GM77014 (D.S.), the Caltech Center for Biological Circuit Design and the Packard Foundation. A.L. acknowledges support from the Fannie and John Hertz Foundation and the UCLA/Caltech Medical Scientist Training Program (NIH GM08042). J.G.O. acknowledges support from the Ministerio de Ciencia e Innovacion (Spain, project FIS2009-13360 and the I3 programme).

Author Contributions D.S. and M.B.E. designed the research. D.S., L.A.S., M.E.F. and G.A.A. built cell lines and performed experiments. D.S., A.L., L.L., J.G.-O. and M.B.E. performed data analysis and mathematical modelling. D.S. and M.B.E. wrote the manuscript with substantial input from the other authors.

Author Information Reprints and permissions information is available at www.nature.com/reprints. The authors declare no competing financial interests. Correspondence and requests for materials should be addressed to M.B.E. (melowitz@caltech.edu).

METHODS

Genetic constructs. We used standard molecular biology techniques to assemble all constructs used in this paper (Supplementary Table 1). The construct used to generate the hN1 cell line, pcDNA3–hN1–mCherry, was constructed by fusing the coding sequence of mCherry to hN1, provided by J. Aster[7]. The construct used to generate the hN1G4^{esn} cell line, pcDNA3–hNECD–Gal4^{esn}, was constructed by replacing amino acids 1742 to 2556 of human NOTCH1 with the amino acids 1–147 and 768–881 of Gal4. The Delta–mCherry fusion consists of the entire coding sequence of rat DLL1 concatenated directly to the coding sequence of mCherry. The reporter for human NOTCH1 activation was constructed from the 12xCSL construct provided by U. Lendahl. The reporter for hNECD–Gal4^{esn} activation was constructed from the UAS construct provided by S. Fraser[5]. Both reporters used a protein fusion of H2B–citrine to localize fluorescence to cell nuclei, where it could be more accurately quantified. Doxycycline-inducible constructs were based on the T-REx system (Invitrogen).

Generation of stable cell lines. All cell lines used in the main text (Supplementary Table 2) were based on the cell line T-REx-CHO-K1 (Invitrogen). Cells were grown in Alpha MEM Earle's Salts (Irvine Scientific) supplemented with 10% Tet System Approved FBS (Clontech), 100 U ml^{-1} penicillin, 100 μg ml^{-1} streptomycin, 0.292 mg ml^{-1} L-glutamine (Gibco) and 10 μg ml^{-1} blasticidin (InvivoGen) at 37 °C in the presence of 5% CO_2 in a humidified atmosphere. Cell lines incorporating multiple transgenes were constructed by sequential rounds of Lipofectamine 2000 (Invitrogen) transfection and selection. Stably transfected clones were generated by limiting dilution or FACS of single cells. Cell lines hN1 and hN1G4^{esn} were first created by stably integrating the 12xCSL–H2B–citrine or UAS–H2B–citrine reporters, respectively, into T-REx-CHO-K1 cells. After selection with media containing 400 μg ml^{-1} Zeocin (Invitrogen) and 10 μg ml^{-1} blasticidin (InvivoGen), individual clones were obtained. Clones with the best dynamic range of reporter induction were identified and used in subsequent stages. pcDNA3–hN1–mCherry or pcDNA3–hNECD–Gal4^{esn} was transfected into the 12xCSL–H2B–citrine or UAS–H2B–citrine reporter cell line, respectively. Cells were selected with media containing 400 μg ml^{-1} Zeocin, 10 μg ml^{-1} blasticidin and 600 μg ml^{-1} Geneticin (Invitrogen). Individual clones were obtained and tested for Notch activity by plating on 2.5 μg ml^{-1} IgG–Delta^{ext}. Clones with minimal background levels and high reporter activation when exposed to Delta were selected and transfected with a plasmid expressing Delta–mCherry under a doxycycline-inducible promoter (pcDNA5–TO–Delta–mCherry). These cells were selected in media containing 400 μg ml^{-1} Zeocin, 10 μg ml^{-1} blasticidin, 600 μg ml^{-1} Geneticin and 500 μg ml^{-1} hygromycin (InvivoGen). Clonal cell populations were obtained, and the clone with the lowest mCherry background expression in the absence of doxycycline, as well as good inducibility of mCherry expression when exposed to 1 μg ml^{-1} doxycycline, was selected for experiments. Cell lines hN1 and hN1G4^{esn} also contain H2B–cerulean under constitutive CMV promoter. A separate cell line containing only inducible Delta–mCherry was created by transfecting T-REx-CHO-K1 cells with pcDNA5–TO–Delta–mCherry. Clones were generated as above, but selection media contained only blasticidin and hygromycin. This cell line was then used to generate the TO–DMC+hN1G4^{esn} cell line by stably transfecting with pcDNA3–hNECD–Gal4^{esn} construct (600 μg ml^{-1} Geneticin).

Experimental techniques and imaging protocols. Surface preparation: All time-lapse microscopy experiments were performed with cells plated on 24-well glass-bottom plates (MatTek). IgG–Delta^{ext} was generously provided by I. Bernstein. For plate-bound Delta experiments, IgG–Delta^{ext} was adsorbed together with 5 μg ml^{-1} hamster fibronectin (Innovative Research) to the glass-plate surface by incubation for 1 h at 4 °C before cell plating. Cells were diluted to 2×10^4 cells ml^{-1} (1×10^5 cells ml^{-1} for co-culture experiments). A calibration was performed to determine the dependence of active IgG–Delta^{ext} concentration on the concentration added during incubation (Supplementary Information).

Preparation of cells for imaging: Before imaging, cells were switched to a low-fluorescence medium consisting of 5% FBS in αMEM lacking riboflavin, folic acid, phenol red and vitamin B12.

Time-lapse microscopy: Movies were acquired using an Olympus IX81-ZDC microscope equipped with an environmental chamber at 37 °C supplying 5% CO_2, a ×20, numerical-aperture-0.7 objective, and automated acquisition software (METAMORPH (version 7.5.6.0), Molecular Devices). For each movie, fluorescence images were acquired in CFP, YFP and red fluorescent protein (RFP) channels, as well as by differential interference contrast microscopy.

Western blot. Western blots were performed using standard protocols. For detection of Gal4, TO–Gal4^{esn} cells were either uninduced or induced for 24 h with 100 ng ml^{-1} doxycycline. We lysed 4×10^6 cells with 200 μl ×1.5 complete SDS loading buffer at 0 h, 1 h, 2 h, 4 h and 6 h after doxycycline removal. Cell lysate (10 μl) was run in triplicate on a NuPAGE Novex 4–12% Bis-Tris Midi Gel (Invitrogen) and transferred to a 0.2 μm nitrocellulose membrane using the Invitrogen iBlot system. The blot was probed with rabbit anti-Gal4 DBD primary antibody (sc-577, Santa Cruz Biotechnology; 1:200) followed by incubation with horseradish peroxidase-labelled anti-rabbit IgG secondary antibody (Amersham; 1:2,000). Bands were quantified using a VersaDoc gel imaging system (Bio-Rad).

Real-time quantitative PCR with reverse transcription. Quantitative PCR with reverse transcription was performed using standard protocols based on the RNeasy kit (Qiagen) and the iScript cDNA synthesis kit (Bio-Rad). RNA was isolated from hN1 and hN1G4^{esn} cells. Complementary DNA was subsequently synthesized from 1 μg of RNA. From a 20 μl reaction, 2 μl of cDNA was used to assess Notch and β-actin mRNA levels.

Flow cytometry analysis of co-cultures. TO–DMC or TO–DMC+hN1G4^{esn} cells were co-cultured with hN1G4^{esn}–No–Delta cells. Cells (1×10^5) were plated at a ratio of 20% Delta cells to 80% Notch reporter cells. Co-cultures were induced by a 12-h pulse of either 1.6 ng ml^{-1} or 100 ng ml^{-1} doxycycline (a well with no doxycycline served as a control). Twenty-four hours after doxycycline removal, co-cultured cells were trypsinized and analysed for YFP fluorescence using a FACScalibur flow cytometer (Becton Dickinson) and standard protocols.

Image and data analysis. Movies were analysed in the following four stages.

Segmentation: Individual cell nuclei were identified in CFP images using a custom algorithm (MATLAB R2007a, MathWorks) based on edge detection and thresholding of constitutively expressed H2B–cerulean fluorescence.

Tracking: For analysis of single-cell expression trajectories, individual nuclei were tracked across frames using custom software (MATLAB, C) based on the softassign algorithm; see Supplementary Information for details.

Verification: All single-cell trajectories were validated using a semi-automated custom software system (MATLAB).

Further detailed analysis: See Supplementary Information.